Sadiq, H., Wong, M.B., Tashan, J., Al-Mahaidi, R. & Zhao, X. L. (2013).
Determination of steel emissivity for the temperature prediction of structural steel members in fire.

Originally published in *Journal of Materials in Civil Engineering, 25*(2), 167-173.

Available from: http://dx.doi.org/10.1061/(asce)mt.1943-5533.0000607

Determination of steel emissivity for the temperature prediction of structural steel members in fire.

H Sadiq[1], *M B Wong*[2], *J Tashan*[3], *R Al-Mahaidi*[4], *X-L Zhao*[5]

Abstract

A numerical method, with which experimental results were processed, was adopted to measure the total emissivity of mild steel specimens at high temperatures. This method is derived from considering the transient thermal energy equilibrium between steel specimen and its surrounding heating environment. As a first step to validate this method, the results obtained at a low temperature were compared with those using infra-red thermographic techniques as recommended in ASTM E1933 and a good correlation of 87% was achieved. The numerical model was then extended to high temperatures to investigate the variation of emissivity of steel with temperatures. The convective heat transfer coefficient being used in the numerical model was examined in great details using results obtained from transient high temperature tests. The emissivity of steel obtained from this study shows that steel emissivity varies over a range of temperatures and the variation becomes more abrupt between 400^{o}C and 500^{o}C, a trend similar to that obtained by Paloposki and Liedquist (2006). Formulation for the emissivity of steel at rising temperatures is recommended for steel design in fire.

[1] PhD Candidate, Dept. of Civil Engineering, Monash Univ., Melbourne, Australia 3800. E-mail: Hussein.Sadiq@monash.edu

[2] Associate Professor, Dept. of Civil Engineering, Monash Univ., Melbourne, Australia 3800 (corresponding author). E-mail: bill.wong@monash.edu

[3] PhD Candidate, Faculty of Engineering & Industrial Sciences, Swinburne Univ. of Technology, Melbourne, Australia 3122. E-mail: Jawdat.Tashan@monash.edu

[4] Professor in Civil Engineering, Faculty of Engineering & Industrial Sciences, Swinburne Univ. of Technology, Melbourne, Australia 3122. Email: Riadh.Al-Mahaidi@monash.edu

[5] Professor in Civil Engineering, Dept. of Civil Engineering, Monash Univ., Melbourne, Australia 3800. E-mail: zhao.xiao.ling@monash.edu

Author keywords: Emissivity; Steel; Temperature; Heat Transfer; Convection; Radiation

Introduction

While steel temperature calculation is straightforward if the total heat flux energy incident on the steel surface is known, the calculation of the total heat flux itself requires accurate thermal properties in relation to mainly the heat convection and radiation process. Specifically, the values of convection and radiation heat transfer coefficients are crucial to the calculation of the total heat flux in an accurate steel temperature prediction process. Furthermore, calculation of heat flux from radiation, which dominates most part of the heat transfer process between fire and steel, requires understanding and careful evaluation of the emissivity in the radiation heat transfer coefficient for both the fire and the steel.

The total emissivity of the surface of a material in fire plays an important role in the radiation part of heat transfer. Measurement of total emissivity of a surface is dependent on physical and thermal properties of the surface such as surface roughness, oxidation, temperature and the heat wavelength at which the measurement is taken (Conroy et al. 1987). It is worth mentioning that the net radiative heat flux equation adopted in the Eurocode is based on the heat transfer theory of two opposite parallel infinite plates where gaseous combustion products are not involved in the heat transfer process. In such a case, determination of the emissivity of steel is required.

For steel substrate, it seems that no consensus on the value of emissivity has been reached and various values have been proposed for adoption by different researchers. SBI (1976) recommends using 0.8 and 0.85 for the steel and fire emissivities respectively, giving a resultant emissivity of about 0.7 for most of the fire test cases considered. Kay et al. (1996) tried to justify a value of 0.8 for the emissivity of steel to be adopted for Eurocode and 0.8 for the fire emissivity, giving a value of 0.64 as the resultant emissivity. Eurocode 3 recommends a value of 0.7 for carbon steel and 0.4 for stainless steel (EN1993-1-2, 2005). The usual practice for steel temperature prediction is to assume a constant value for the steel emissivity in order to match experimental results, although it has been known that steel emissivity may vary with temperature (Wong and Ghojel 2003a).

Indeed, it has been shown that the use of a constant value of total emissivity for steel temperature prediction would not match all the experimental results (Smith and Stirland 1983, White et al. 1999). Ghojel (1998) proposed a heat transfer model to predict the temperature of steel structure in a fire compartment by accounting for the variable emissivity and absorptivity of the gaseous composition of the combustion products in a fire. A good agreement was achieved with the proposed model in comparison with reported experimental data. In the current study, temperature rise for steel specimens was recorded in an electric heated furnace and therefore the emissivity formulation proposed by Ghojel (1998) no longer applies.

Calorimetric and optical methods can be adopted to measure the emissivity of surfaces (Moghaddam et al. 2007). However, special care should be taken while using these methods. For calorimetric methods, the specimens should be insulated from most of its sides to prevent any parasitic heat transfer and, for optical methods; the measurement should be taken from different angles. Both methods involve intensive labour and practical difficulties that are hard to overcome in standard laboratories (Moghaddam et al. 2007). Moreover, those methods give only one measured value of emissivity for a specific temperature and can only be used for a limited temperature range. The maximum attaining temperature in most existing methods is about 300°C which is a very modest temperature compared to the maximum temperatures required in fire tests for steel fire design.

Paloposki and Liedquist (2006) proposed an indirect method to measure the total emissivity of metallic substrates at high temperatures using the thermal energy equilibrium on a surface. The proposed method is very simple and does not need sophisticated equipment to be used. However it is applicable for objects with high thermal conductivity such as metals in which the temperature profile along the thickness should be uniform. The method was based on maintaining a constant temperature inside the furnace prior to the commencement of the fire test. It was therefore limited to a minimum temperature of about 150ºC and reliable results were not possible below this temperature as the constant temperature regime was disturbed when the furnace door was opened for installing the test specimens. Good agreements were found between this method and another optical method at 200ºC conducted for two types of stainless steel; however this was not the case for carbon steel specimens. Moreover, in their experiments, the constant temperature was kept at 700^{o}C giving a very high heating rate for the test specimens.

In the current study, the method to find the emissivity of carbon steel surface is similar to that used by Paloposki and Liedquist. The process of heating the specimens was modified and in this instance the specimen was placed in the furnace prior to the test so that both the furnace and the specimen temperatures were continuously and simultaneously monitored and measured without any disturbance. As a first step to validate this method, the results obtained at a low temperature were compared with those using infra-red thermographic techniques as recommended in ASTM (ASTM E 1933-99a, 2005) and a good correlation was achieved. The sensitivity of this method against variables including the size of the time interval taken to solve the energy equation and the convective heat transfer coefficient was also investigated. The numerical procedure is adopted from a previous study by Wong and Ghojel (2003b).

Finally, formulation for the emissivity of steel is recommended for use in high temperature steel design.

Methodology

Convection Heat Transfer Coefficient

Three main factors influence the convection heat transfer coefficient. These are the geometry of the surface on which heat energy is incident, the conditions of the heat flow and the temperature between the specimen and its environment (Moran et al. 2003). By knowing the geometry of the surface and identifying the flow condition as free or forced convection, laminar or turbulent flow along the surface, appropriate dimensionless correlations can be obtained to find the convective coefficient. The important parameters in establishing such correlations are the Nusselt (Nu_L), Reynolds (Re_L), Prandtl (Pr) and Rayleigh (Ra_L) numbers. For the characterization of free convection, Grashof number (Gr_L) is also used.

Nusselt number represents the slope of the temperature at the surface of the object and directly correlates the surface convection coefficient as shown in Eq. (1):

$$h_c = \frac{Nu_L k}{L} \tag{1}$$

where h_c and L are the convective heat transfer coefficient and the characteristic length of the surface respectively; for rectangular horizontal plate, L= Surface area/surface perimeter and k is the thermal conductivity of the environment in (W/m K). Also Nusselt number is presented as a function of Rayleigh and Prandtl numbers in free convection. According to the case considered as free convection in this study, the Rayleigh and Nusselt correlations used in the analysis are for a horizontal cylinder and $L = D$, the diameter of the cylinder:

$$Ra_D = \frac{g\beta(T_f - T_s)D^3}{\nu\alpha} \tag{2}$$

$$Nu_D = \left\{ 0.60 + \frac{0.387 Ra_D^{1/6}}{\left[1 + \left(\frac{0.559}{\mathbf{Pr}} \right)^{9/16} \right]^{8/27}} \right\}^2 \text{, } Ra_D \leq 10^{12} \tag{3}$$

where

g is the acceleration of gravity (= 9.81 m/s^2)

β is the volumetric thermal expansion coefficient (K^{-1}) and can be taken as:

$$\beta = \frac{1}{\frac{(T_s + T_f)}{2} + 273} \tag{4}$$

v, α and Pr are the respective momentum diffusivity, the thermal diffusivity and Prandtl number which is the ratio of the momentum and thermal diffusivities of the furnace medium. T_s and T_f are the specimen and the furnace temperatures (ºC) respectively. The thermo-physical properties of the air as a function of temperature were taken from Moran et al. (2003). The values of these parameters were used to find the coefficient of heat convection for the furnace by applying Eqs. (1) to (4).

The convective heat transfer from the heated environment in the furnace to the specimen is given by

$$q_{conv} = h_c(T_f - T_s) \tag{5}$$

Radiation Heat Transfer Coefficient

The radiation exchange between a heated object, such as a small steel specimen, at temperature T_s, and a large isothermal surrounding, such as the furnace walls at temperature T_f, is represented by the net radiation equation:

$$q_{net\,rad.} = \alpha \cdot \sigma \cdot T_f^{\ 4} - \varepsilon \cdot \sigma \cdot T_s^4 \qquad (6)$$

where α, ε and σ are the total absorptivity, the total emissivity of the specimen surface and Stefan Boltzmann constant (5.67×10^{-8} W/m^{2}K^4) respectively. One of the essential assumptions of gray surface is that the total emissivity is equal to the total absorptivity and both are independent of the wavelength. Hence:

$$q_{net\,rad.} = \varepsilon \cdot \sigma \left(T_f^4 - T_s^4\right) \qquad (7)$$

In general, it is a practical assumption that insulated walls in furnace are treated as gray surfaces in order to simplify the analysis process (Moran et al. 2003). The net radiative heat flux given in Eq. (7) is a special case of the general equation accounting for the view factor between the two surfaces. Equation (7) is applicable when the surface area of the object is very small compared to the area of the enclosure (Moran et al. 2003), as is the case of the current study.

If an object is placed in a furnace, the change of energy storage due to the temperature change is equal to the energy flow due to convection and net radiation. Thus,

$$E_{st} = E_{in} - E_{out} = \dot{q}_{net} \qquad (8)$$

where E_{st} is the rate of increase or decrease in the internal energy of the object usually corresponding to an increase or decrease in temperature and $\dot{q}_{net}$ is the net heat flow into the object due to convection and radiation. Mathematically,

$$E_{st} = \frac{dU}{dt} = c_p m \frac{dT_s}{dt} \tag{9}$$

which, when combined with Eqs. (5) and (7), can be written as

$$c_p m \frac{dT_s}{dt} = A\left[h_c (T_f - T_s) + \varepsilon\sigma(T_f^4 - T_s^4)\right] \tag{10}$$

where c_p, m and A are the specific heat, the mass and the surface area of the object respectively. The term dT_s/dt is the heating rate of the specimen. Assuming that the metallic specimen is inert at a range of temperatures within which its emissivity is to be measured, the energy balance equation can be rearranged at a transient time of heating to obtain the emissivity indirectly as

$$\varepsilon(T) = \frac{c_p \rho \frac{V}{A}\frac{dT_s}{dt} - h_c (T_f - T_s)}{\sigma\left(T_f^4 - T_s^4\right)} \tag{11}$$

where ρ and V are the density and the volume of the tested specimen respectively.

Experimental Procedures

High Temperature Test

Equation (11) can be used to obtain the variation of steel emissivity with temperature if a set of values for T_f and T_s are available over a practical range of temperatures. Thus a high temperature test was performed on a steel rod.

An electrical furnace with 800×350×350 mm internal dimensions was used for the high temperature test as shown in Fig. 1. To verify the validity of Eq. (1) for the evaluation of the convective heat transfer coefficient, a comparative test was first performed. Two rod specimens, one made of nickel titanium (NiTi) alloy and the other carbon steel, were prepared with identical dimensions of 10 mm in diameter and 200 mm in length. The purpose of using specimens with different materials was to examine the effect of different thermal properties on the convective coefficient. Two thermocouples were used for each specimen, one to monitor the surface temperature and the other to monitor the temperature of the surrounding environment in the vicinity of the specimen. Special care was taken to mount the thermocouple on to the specimen surface in order to minimise the effect of the heat flux intercepted directly by the thermocouple sensor. This was done by covering the thermocouple with ceramic fibre tape as an insulation material as shown in Fig. 1.

Infra-Red Thermography Test

To validate the parameters used to calculate the emissivity of the steel specimen in Eq. (11), an alternative method based on thermographical technology was used to obtain its emissivity at a low temperature of 60^{o}C. The ASTM E 1933 method of applying the infra-red technique to obtain the emissivity is adopted in this study (ASTM E 1933-99a, 2005). For calibration purposes, a portion of the steel specimen’s surface was painted black to simulate a blackbody which has a known emissivity. This was done by spraying a flat black paint on half of the specimen. Figure 2 shows the steel surface modified for the infra-red test.

The infra-red radiation can be detected by special equipment with sensors, type PU11 T from Hukseflux Thermal Sensors Company. These sensors can generate electrical signals in proportion to the amount of received infra-red radiation. The equipment has a computational functioning unit which can convert the reading of the sensors to temperature. The applications of the non-destructive infra-red thermography depend very much on the abilities and specifications of these infra-red sensors.

Infra-Red camera

A NEC Thermo Tracer TH9260 thermal camera from NEC Avio Infrared Technologies is used to measure the emissivity in this study. This camera operates in the medium-long wavelength infra-red spectral band between 8 μm and 13 μm. It has a thermal sensitivity of 0.06^{o}C at 30^{o}C. The measurement accuracy is ± 2^{o}C or 2% of the reading at ambient temperature of 0^{o}C ~ 40^{o}C. The detectable measurement is up to 30 frames per sec. This detector has an uncooled focal plane array (FPA) microbolometer detector with 640 (Horizontal) × 480 (Vertical) pixels. The minimum detectable area that this imager can detect is 0.18 mm^2. The emissivity input correction is between 0.1 and 1.0. The detector is provided with ambient temperature correction, background temperature correction, and distance from object correction. The calibration of the camera was done by the manufacturer. The camera is supported with many image processing functions and can read temperatures for different points and provides the infra-red reading with different shapes as regions of interest. The data can be recorded with real time interval measuring.

According to Planck's Law, as objects with high temperature emit radiation in short wavelengths, the detector with long wavelength received radiation with minimal atmospheric effects. For that, the TH9260 infra-red detector has showed minimum noisy images.

The obtained data was digitized and displayed as shades of colour or gray colour with many different patterns. The controlling of these displaying patterns can enormously affect the detection process. Cooler or hotter regions of interest are identified by a different shading colour when compared with the neighbouring areas.

Test setup

The NEC camera was positioned at 1 metre from the specimen. To confirm that the temperature differences in the infra-red records are not due to the reflections on the steel surface, a digital video camera is used in parallel with the TH9260 infra-red detector to provide a record of the regions of interest to monitor and compare the infra-red and the visual captures. Moreover, the test was conducted under a background of black curtains to minimize the reflections on the steel surface. The infra-red camera was connected to computer in video mode.

Infra-red software *Image Processor ProII* version one 2009 from NEC was used. This software works in two modes: online when the camera is connected to the PC, or offline when it is not. The package has different advanced capabilities providing different digital video framing rates and image acquisition and analysis. Parametric adjustments of the data processing unit were performed according to the thermal properties of the blackbody. The camera was pointed at the steel surface. Under digitalized infra-red readings, IR images were recorded and monitored on both modified and original portions of the steel specimen's surfaces. The known emissivity of the blackbody was input in the IR software for the modified steel portion. Then emissivity of the original steel surface was obtained by adjusting the input value of the emissivity until the IR camera detects the same temperature of the modified steel surface. This process was repeated three times and the average emissivity reading was recorded.

Results and Discussions

Infra-Red Test

To obtain a valid image using the infra-red imaging technique, the steel specimen needs to be at least 10°C hotter or cooler than the ambient temperature (ASTM E 1933-99a, 2005). A tungsten halogen light lamp from IANIRO was used to provide this temperature difference between the specimen and the ambient. The maximum capacity of the light was 2000 watts.

Figure 3 shows the infra-red image for the steel specimen. As illustrated in the diagram, the thermograms show differences in temperatures between the specimen and the ambient and between the modified and original surfaces of the specimen. The emissivity of the steel specimen was measured at 60.3ºC and the readings were between 0.29 and 0.32. This process was repeated five times and the average emissivity reading was found to be 0.3.

High Temperature Test

Figure 4 depicts the temperature history of the two specimens and the environment. There is a slight temperature difference of about 25ºC in the environment recorded by the two thermocouples, Furnace(steel) and Furnace(NiTi), for each of the specimens even though they were placed relatively close to each other. This implies that there was a small temperature gradient in the space of the furnace. Nevertheless, for analysis purposes the environment temperature for each specimen was taken separately according to the temperature recorded by the thermocouple adjacent to it.

Also from Fig. 4, it is observed that the furnace does not follow the standard ISO834 fire curve which has a higher heating rate and may not be ideal for the current study. As a result of the different thermal properties for the NiTi and the mild steel materials, temperature histories of steel and NiTi specimens were not the same although they had the same geometry and were exposed to a similar environment simultaneously. In Fig. 4, both the NiTi alloy and the steel temperature-time curves possess a small plateau where the temperatures do not increase significantly. It is around 100°C for the NiTi alloy and 700°C for the steel. The reason behind this phenomenon is that NiTi alloy and steel experience solid to solid phase transformation at around 100ºC and 700ºC respectively and most of the incident heat energy is consumed by the transformation.

Convective coefficient

The formulation described for heat transfer in this study is generally applied to a steady state heat transfer problem whereas the conducted test is a transient heat transfer problem. To apply the equations to the test results, the time duration of the test, about 28 minutes, was divided into small time intervals, Δt = 10 seconds. Spreadsheet method (Wong and Ghojel 2003b) was applied at the end of each interval to calculate the convective coefficient based on the specimen and the environment temperatures using the appropriate equations. The thermo-physical properties of the air, namely v, α and Pr, were obtained using the average temperature of the specimen and the furnace environment at the end of each time interval. These thermo-physical properties are required in the calculations of Eqs. (1) to (4) as mentioned previously. Table 1 demonstrates the sequence of the calculations to obtain the convective coefficient, h_c, using temperatures of the furnace and the steel measured experimentally. Temperatures recorded below the 49°C steel temperature are neglected in the calculations because heat energy was not consistent around the specimen and that may lead to spurious numerical results. Only part of the data is presented in Table 1 to demonstrate the calculation of the convective coefficients.

Figure 5 shows the calculated coefficient of heat transfer by convection, h_c, as a function of furnace temperature. Coefficients calculated from NiTi alloy and mild steel specimens show a good agreement especially at temperatures from 25°C to around 400°C even though there was a noticeable difference in their surface temperature over this range during the test. NiTi alloy produced an average convective coefficient of 10.5 W/m^{2}K and the mild steel specimen an average of 10.8 W/m^{2}K. It should be noted that convective coefficient usually does not have a constant value because it is, amongst other conditions, a function of the temperature difference between the specimen and the furnace environment.

Emissivity of steel

To obtain the total emissivity, ε, of carbon steel, the temperature data of the tested steel rod were used. The specific heat variation of the steel with temperature was taken as that recommended in EC3 (EN1993-1-2, 2005) and the convective heat transfer coefficient obtained from the previous section was used in this analysis. Spreadsheet method was adopted to solve the energy equilibrium equation at time steps of 10 and 20 seconds. Table 2 shows the steps that are required to calculate the steel emissivity using the measured steel and environment temperatures, the convective coefficients obtained from Table 1 and Eq. (11). Once again the calculations start at steel temperatures above 49°C to avoid any numerical noises arising from the inconsistency in the heat energy below this temperature and only part of the data is presented in Table 2 to demonstrate how the calculation is carried out.

Figure 6 depicts the variation of the calculated total emissivity with the specimen temperature. When compared with the result from the infra-red test at 60.3ºC, this method slightly underestimates the total emissivity but in general gives a good agreement. Table 3 compares the results obtained from the two methods at 60.3°C at which the method based on Eq. (11) agrees with the infra-red method to 87%. Figure 6 shows the variation of the total emissivity between 50ºC and 600ºC of the specimen temperature. This range of temperatures was selected from a practical point of view because steel loses most of its strength at temperatures above 600ºC.

Figure 6 also shows that the method is not sensitive to the magnitude of the time interval. There are two temperature ranges within which the total emissivity is almost a constant. One is from 50ºC to around 400ºC and the other from 500ºC to 600ºC. However, a rapid increase in the total emissivity occurs from 400ºC to 500ºC. The reason for such rapid increase is that the specimen surface starts to oxidise and changes surface roughness, roughens , causing a change of the total emissivity from around 0.28 at 50ºC to around 0.7 at 600ºC. From the literature, the total emissivity of carbon mild steel with freshly rolling surface is usually in the realm of 0.2-0.32 at room temperature (Croft and Stone 1977, Tanaka et al. 1989).

In many steel design applications, the convective coefficient is always assumed to be a constant. To demonstrate the effect of such assumption, a comparison study was performed to evaluate the total emissivity of steel. Figure 7 gives a comparison between the total steel emissivity values, ε, calculated from using the variable convective coefficient shown in Fig. 5 and those obtained from using an average value of 10.8 W/m^2 K. From the figure, it can be seen that there is a significant difference in the results of emissivity obtained from these two methods at low temperature range. As the temperature increases, the total emissivity with constant convective coefficient starts to converge to that obtained from variable convection factor. There is a good match at temperatures above 400ºC. At high temperatures, the difference is minimal as radiation dominates the heat transfer process in this temperature range.

Recommendations

Numerical procedure is often used in temperature prediction for steel design under high temperatures. Computational tools such as spreadsheet are commonly adopted to carry out the numerical procedure efficiently. As the procedure involves incremental time steps in a sequential order, it is ideal to adopt spreadsheet functions for this purpose. Thus, a numerical model simulating the thermal behaviour of the steel member requires formulations to represent the parameters used in the numerical procedure. The results obtained from this study for the emissivity of steel can be conveniently cast into a formulation for such computations.

The variation of the emissivity with temperature T can be divided into three main temperature regions:

For $T < 380^{o}C, \varepsilon = 0.28$. (12a)

For $380^{o}C \leq T < 520^{o}C$, $\varepsilon = 0.00304T - 0.888$. (12b)

For $520^{o}C \leq T$, $\varepsilon = 0.69$. (12c)

A plot of Eq. (12) together with the results obtained from the proposed method are shown in Fig. (8), the test results obtained by Paloposki and Liedquist (2006) are also shown in the figure for the comparison purposes. The current investigation covers a wider temperature range with more stable results compared to that obtained from Paloposki and Liedquist (2006).

Conclusions

A simple and efficient method to find the emissivity of a steel surface based on both numerical analysis and experimental investigation is presented in this study. The current investigation is different to the one by Paloposki and Liedquist (2006) in that: (a) the current method is based on a continuous heating regime with steady increasing temperature without interruption, thus enabling a complete practical temperature range for structural steel to be evaluated; (b) a thorough investigation into the validity of the convective heat transfer coefficient was conducted; (c) a reliable infra-red thermography method was used to validate the parameters being used in the current formulations for heat transfer at low temperature and a good agreement of 87% was achieved between the current proposed method, Eq. (11), and the infra-red method at 60.3°C, whereas the SP results obtained by Paloposki and Liedquist (2006) were inconsistent with experimental data for carbon steel; (d) a simple formulation is proposed for emissivity of carbon steel to be used in structural fire design. In general, the total emissivity of steel has been found to vary between 0.28 to 0.69 within a temperature range of 380^{o}C and 520^{o}C.

The current method is only applied to materials that have high thermal conductivity such as steel. The method has been found to be insensitive to the magnitude of the time step employed to solve the energy equilibrium equation. The convective coefficient has a major impact on the credibility of the method; a constant value of the convective coefficient would not give reliable results especially at low temperatures at which heat transfer by convection dominates the heating process. Rather, it is recommended to use convective coefficient calculated from the fundamental principles. The convective coefficient has been found to vary with temperature. The formulation proposed for describing the variation of emissivity with temperature is suitable for general heat transfer computations and is recommended for adoption in structural fire design of steel structures.

References

ASTM E 1933-99a (2005). "Standard Test Method for Measuring and Compensating for Emissivity Using Infrared Imaging Radiometers."

Conroy, C., Guthrie, J., Sharkins, A., Sparr, B., Crocombe, R., and Curbelo, R. (1987). "An infrared accessory for studying the emissivity of aluminum surfaces." *Applied Spectroscopy*, 41(4), 688-692.

Croft, D., and Stone, J. (1977). *Heat transfer calculations using finite difference equations.*, Applied Science Publishers, Barking, UK.

EN1993-1-2 (2005). "Eurocode 3: Design of steel structures-Part 1-2: General rules-structural fire design. " CEN, Brussels.

Ghojel, J. (1998). "A new approach to modeling heat transfer in compartment fires." *Fire Safety Journal*, 31(3), 227-237.

Kay, T., Kirby, B., and Preston, R. (1996). "Calculation of the heating rate of an unprotected steel member in a standard fire resistance test." *Fire Safety Journal*, 26(4), 327-350.

Lienhard, J. H. (2003). "A Heat transfer Textbook." *Pholgiston Press*, 3rd edition.

Moghaddam, S., Lawler, J., Currano, J., and Kim, J. (2007). "Novel Method for Measurement of Total Hemispherical Emissivity." *Journal of Thermophysics and Heat Transfer*, 21(1), 128.

Moran, M., Shapiro, H., Munson, B., and DeWitt, D. (2003). *Introduction to thermal systems engineering*, Wiley.

Paloposki, T., and Liedquist, L. (2006). "Steel emissivity at high temperatures; http://www.nordicinnovation.net/nordtestfiler/rep570.pdf, accessed 11 May 2011.".

SBI (1976). "fire engineering design of steel structures." *Swedish Institute of Steel Construction*.

Smith, C., and Stirland, C. (1983). "Analytical methods and the design of steel framed buildings." *International Seminar on Three Decades of Structural Fire Safety, Fire Research Station, Herts, UK*, 155-200.

Tanaka, F., Ohira, H., and Naganuma, Y. "Application of a new radiation thermometry method to galvannealed and cold-rolled steels." IEEE, 24-28.

White, D. A., Beyler, C. L., Scheffey, J. L., and Williams, F. W. (1999). "Modeling the impact of post-flashover shipboard fires on adjacent spaces." *Journal of Fire Protection Engineering*, 10(4), 2.

Wong, M., and Ghojel, J. (2003a). "Sensitivity analysis of heat transfer formulations for insulated structural steel components." *Fire Safety Journal*, 38(2), 187-201.

Wong, M., and Ghojel, J. (2003b). "Spreadsheet method for temperature calculation of unprotected steelwork subject to fire." *The Structural Design of Tall and Special Buildings*, 12(2), 83-92.

Table 1. Calculations of h_c using spreadsheet method

Δt	T_s	T_f	$(T_f+T_s)/2$	β Eq. (4)	ν $\times 10^{-5}$	k	α $\times 10^{-5}$	P_r	Ra_D Eq. (2)	Nu_D Eq. (3)	h_c Eq. (1)
s	°C	°C	°C	K^{-1}	m^2/s	W/m.K	m^2/s	No.	No.	No.	$W/m^2.K$
10	48.9	215.8	132.3	0.0024	2.36	0.0341	3.63	0.68	4710.7	3.65	12.4
10	52.2	224.8	138.5	0.0024	2.43	0.0345	3.72	0.68	4547.5	3.62	12.5
10	55.6	233.3	144.4	0.0024	2.5	0.0350	3.80	0.68	4385.0	3.59	12.5
10	59.1	241.7	150.4	0.0024	2.57	0.0354	3.89	0.68	4224.4	3.56	12.6
10	62.8	250	156.4	0.0023	2.64	0.0358	3.98	0.68	4062.2	3.53	12.6
10	66.5	257.7	162.1	0.0023	2.71	0.0362	4.07	0.68	3907.7	3.50	12.6

Table 2. Calculations of steel emissivity, ε, using spreadsheet method

Δt	T_s	T_f	h_c	c_p	$\Delta T_s/\Delta t$	ε Eq. (11)
s	°C	°C	W/m^2.K	J/kg°C	°C/s	
10	45.7	206.6	12.4	457.0	-	-
10	48.9	215.8	12.4	459.02	0.32	0.278
10	52.2	224.8	12.5	461.06	0.33	0.264
10	55.6	233.3	12.5	463.14	0.34	0.255
10	59.1	241.7	12.6	465.24	0.35	0.248
10	62.8	250	12.6	467.43	0.37	0.268
10	66.5	257.7	12.6	469.58	0.37	0.241

Table 3. Average steel emissivity results obtained from Eq. (11) and infrared test

Test	T_s (°C)	ε (Mean)	Standard deviation	Coefficient of variation
Infra-Red	60.3	0.3	0.0114	0.0375
Eq. (11)	60.3	0.26	0.025	0.0956

Fig. 1. Interior view of the furnace with NiTi alloy and carbon steel specimens

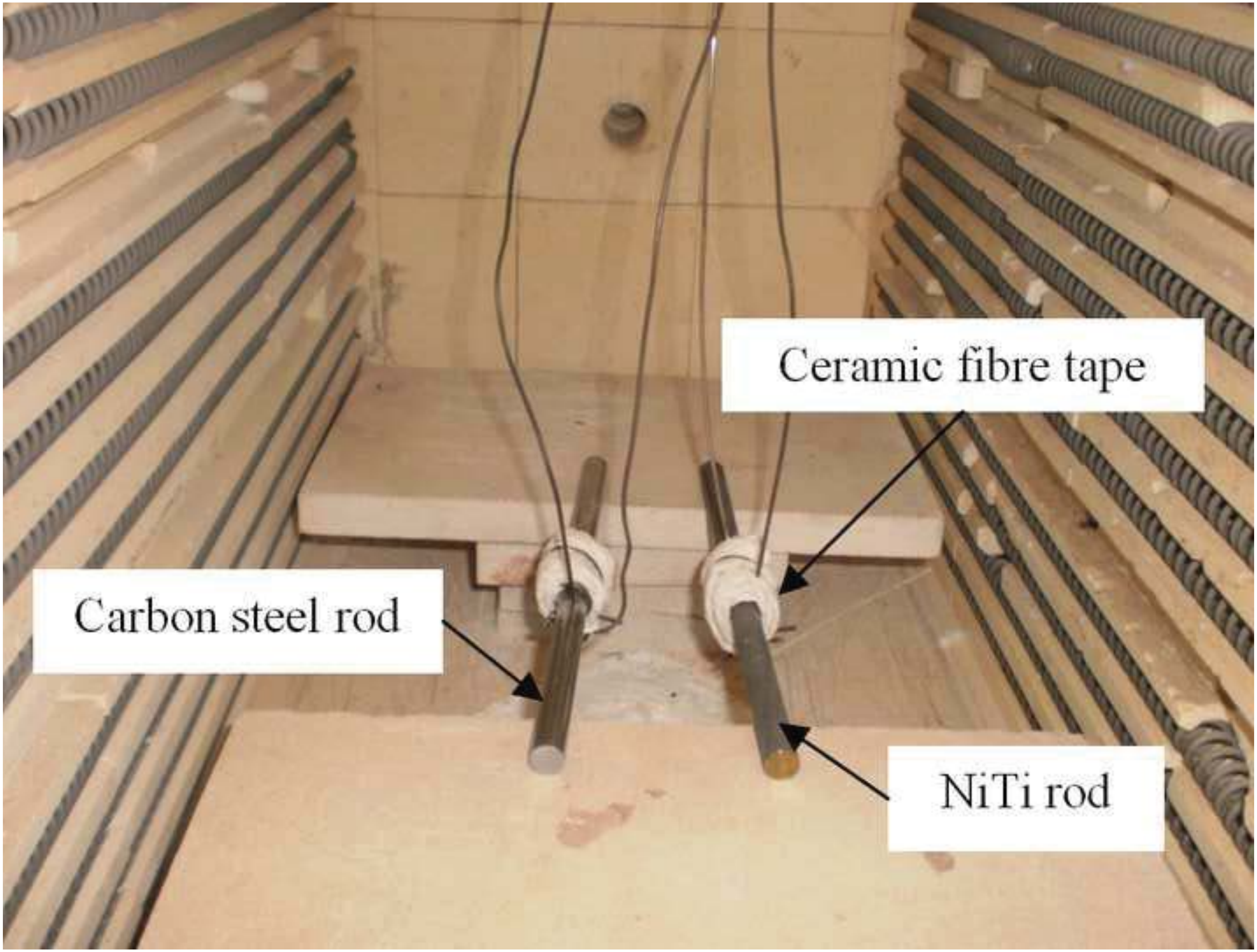

Fig. 2. Steel specimen with portion of the painted surface

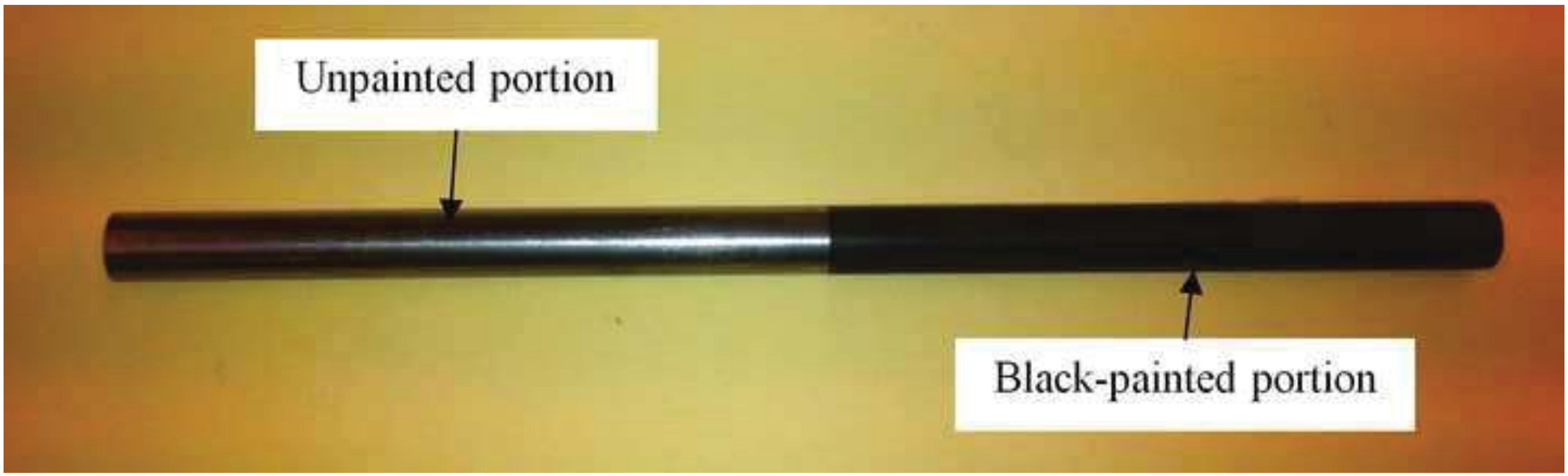

Fig. 3. Infra-Red image of the heated specimen

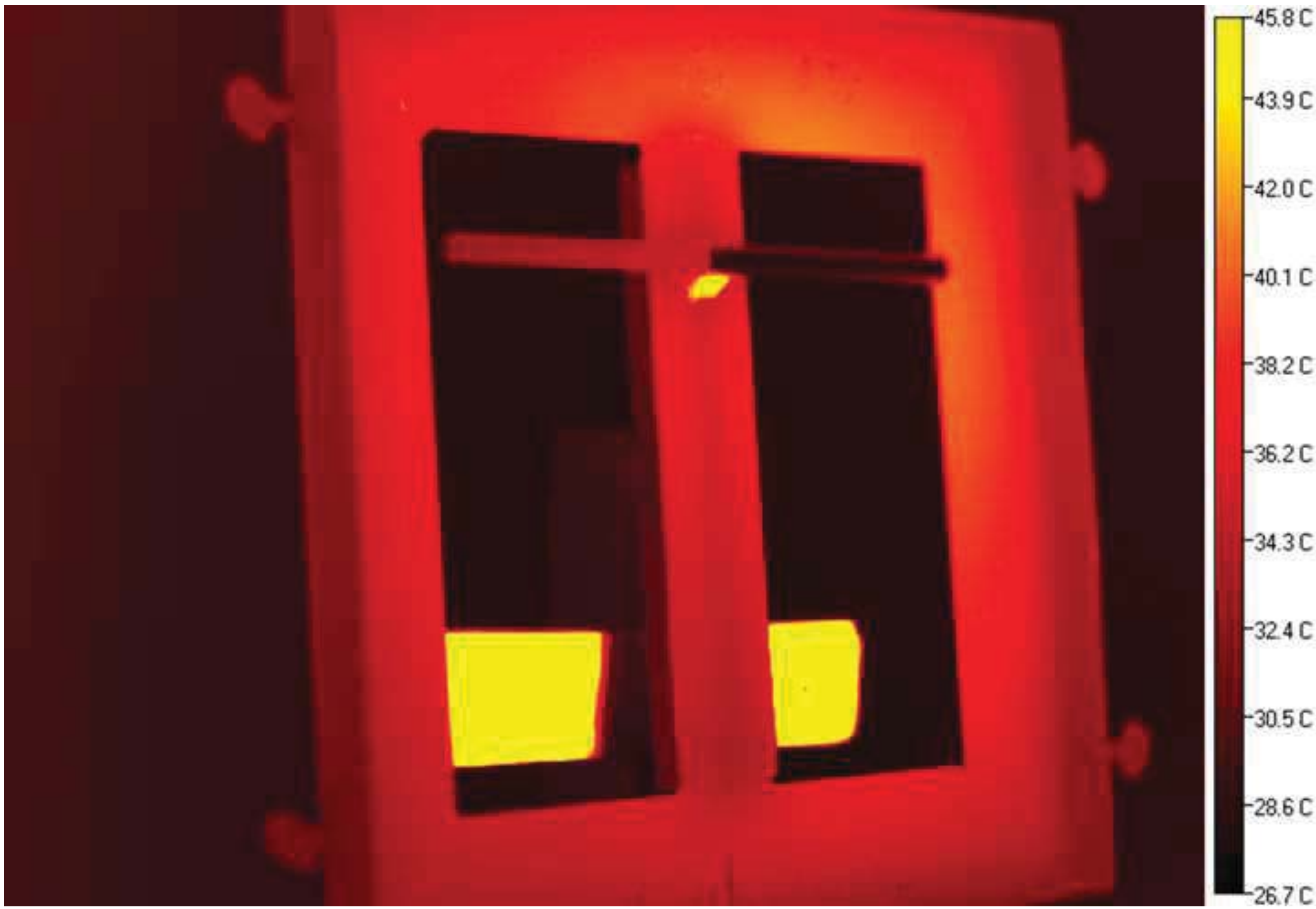

Fig. 5. Values of convective coefficient for the electrical furnace

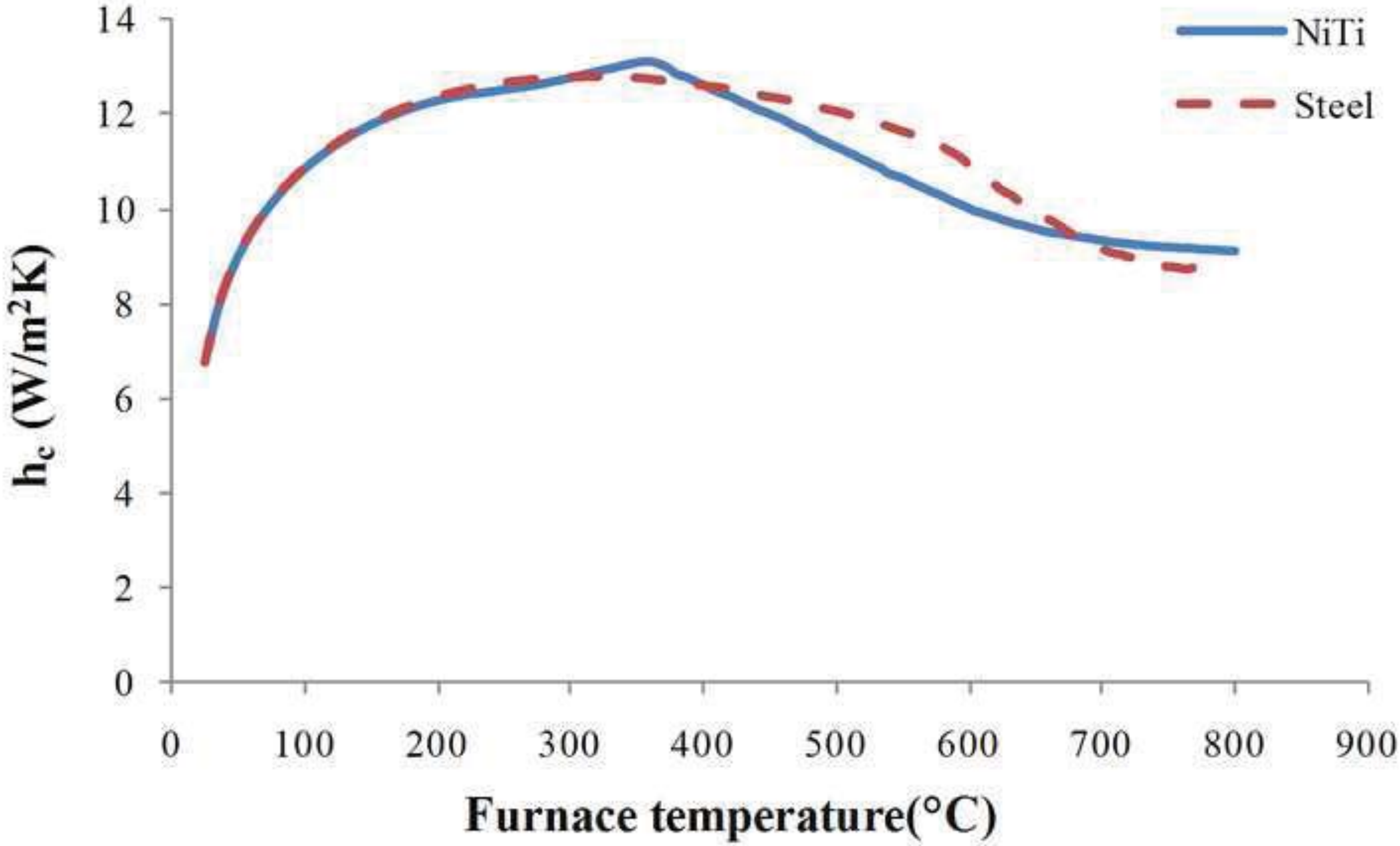

Fig. 6. Total emissivity values of steel as a function of specimen temperature

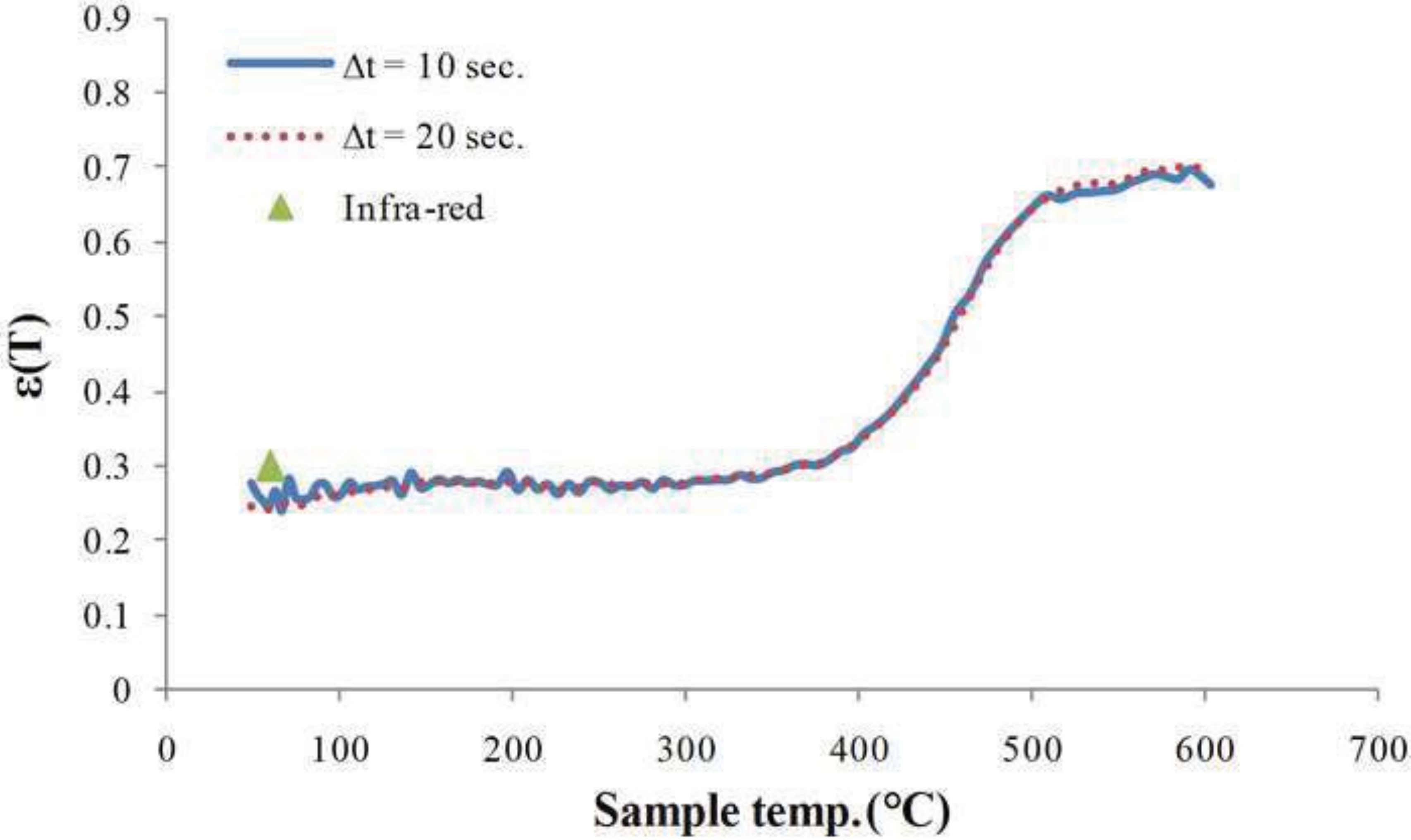

Fig. 7. Total emisiivity values of steel using constant and variable convective coefficients

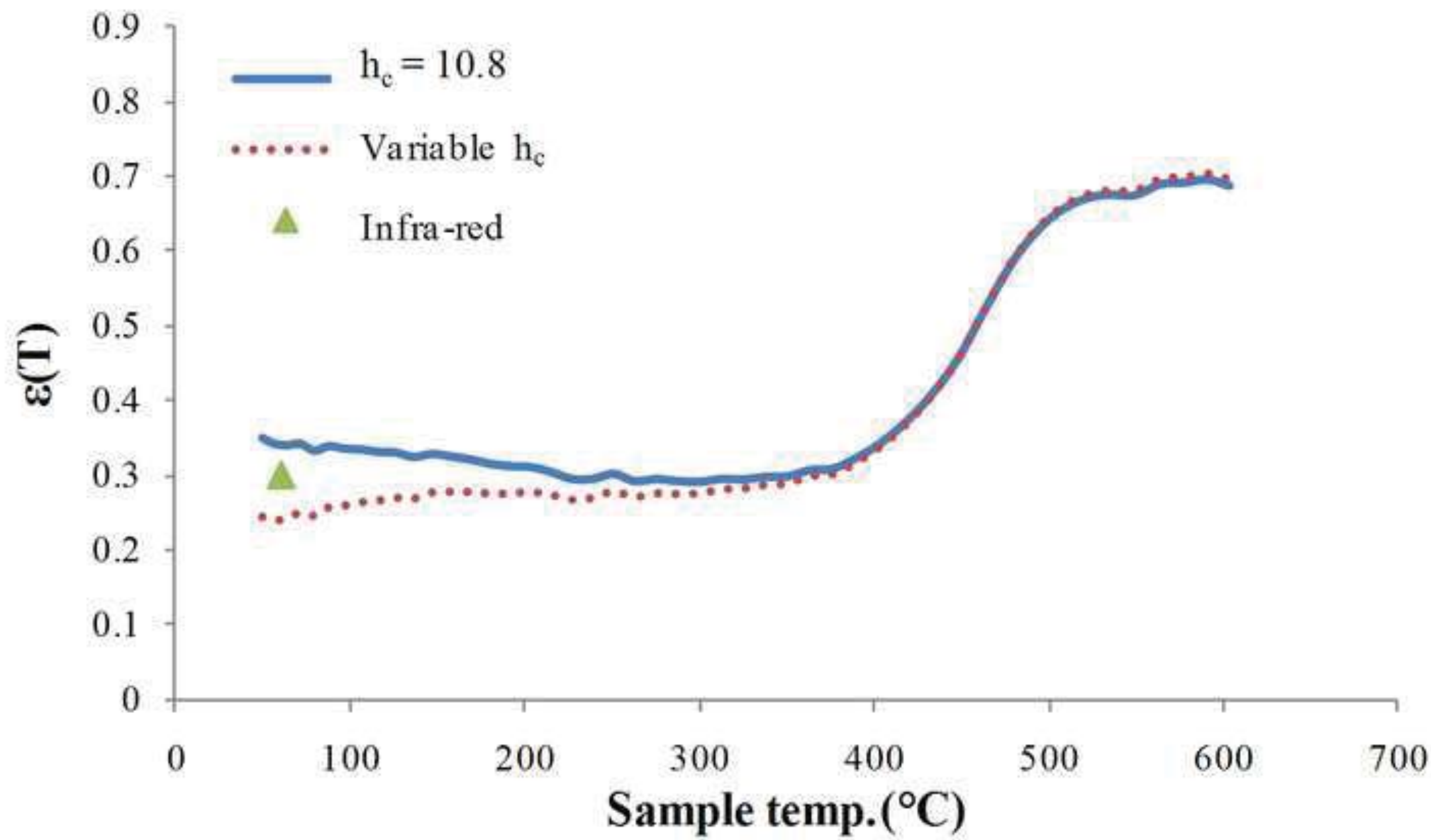

Fig. 4. Temperature-time response of NiTi alloy and mild steel specimens

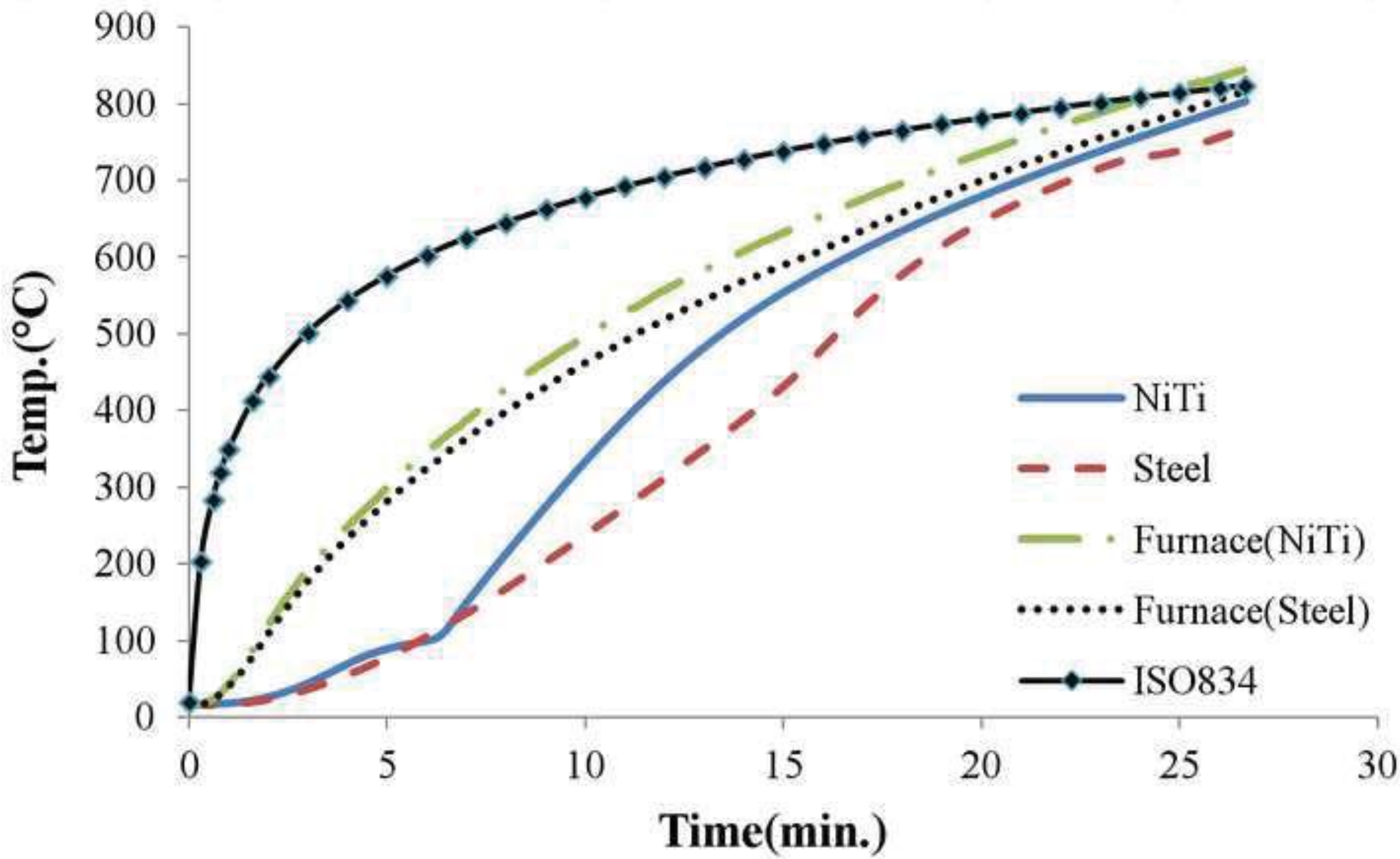

Fig. 8. Steel emissivity simulation and test results